ISSN 0016-7029, Geochemistry International, 2007, Vol. 45, No. 7, pp. 698–716. © Pleiades Publishing, Ltd., 2007.
Original Russian Text © V.Yu. Rusakov, 2007, published in Geokhimiya, 2007, No. 7, pp. 766–785.

Comparative Analysis of the Mineral and Chemical Compositions of Black Smoker Smoke at the TAG and Broken Spur Hydrothermal Fields, Mid-Atlantic Ridge

V. Yu. Rusakov

Vernadsky Institute of Geochemistry and Analytical Chemistry, Russian Academy of Sciences, ul. Kosygina 19, Moscow, 119991 Russia

e-mail: rusakov@geokhi.ru

Received August 17, 2005

Abstract—The paper presents newly obtained data on the fluxes of hydrothermal–sedimentary material collected with sedimentation traps within 3 m from the bottoms of black smokers at the TAG and Broken Spur hydrothermal fields and reports the results of comparative analysis of the mineralogical and chemical compositions of this material. The sedimentary material deposited near the vent was determined to account to approximately 3% of the overall mass of the orebody. The results demonstrate that, in both cases, the trap material is characterized by high contents of ore components and ore-forming chemical elements (Fe, Cu, Zn, and Co), and Se, As, Sb, Ba, and P compared to tholeiitic basalts from which these elements are leached. However, the material of a more "mature" (having an age of 40–50 ka) hydrothermal spring at the TAG field contains 40% Fe hydroxides, in contrast to the material of a spring at the Broken Spur field (age <1000 yr) whose material is dominated by sulfides (72%) and contains much pyrrhotite. These springs also show principal differences between the enrichment coefficients for Se (by a factor of 4.8), As (3), Ca (4.1), and Si (5.2). These differences are thought to reflect various evolutionary stages of the circulating hydrothermal systems.

DOI: 10.1134/S0016702907070063

INTRODUCTION

Hydrothermal–sedimentary material produced when hydrothermal solutions interact with seawater forms contained not only metalliferous sediments outside hydrothermal fields but massive sulfide ores in the immediate vicinity of the vents also. It is, however, quite difficult to unambiguously assay its role in the origin of orebodies. First, only unsystematic and scarce data are currently available on the composition of this material and its fluxes, because the sampling of particles precipitating in the close vicinity of hydrothermal vents, which usually occur at depths of more than 2 km, is still a technically complicated problem, whose solution is thus fairly expensive. Second, the processes forming this material itself are poorly understood as of yet. It is absolutely unclear whether the composition of the hydrothermal–sedimentary material should vary during the evolution of a submarine hydrothermal system.

As follows from the results obtained by studying known submarine hydrothermal ore mineralization, the accumulation of their ore material from the feeding hydrothermal solutions (fluids) poured out at the seafloor at the discharge areas of recycling hydrothermal systems is characterized by a complicated history and often cannot be interpreted unambiguously. The various viewpoints are mostly underlain by the following two major approaches. One of them proceeds from the assumption that various spatially separated mineral assemblages can be formed by a single solution depending on local thermochemical conditions. The other approach assumes that ores were successively formed by solutions that chemically evolved with the evolution of the hydrothermal system. Another more complicated thermodynamic model combines the mechanisms of the deposition of ore material in the course of cooling of the high-temperature fluid with seawater, an evolutionary change of the chemistry of the fluid, and metasomatic replacements within a single ore edifice [1]. However, considering the cyclic character of hydrothermal activity [2] and the polygenetic nature of the sulfide ore mineralization [3], it is difficult to unambiguously trace the evolution of ore accumulation using the mineralogy of the ore edifice as the only indicator. Massive sulfide ores are variably affected by the later recrystallization of the material under the effect of metasomatic processes. The importance of the utilization of the hydrothermal-metasomatic material as one of the indicators of the evolution of ore deposition notably increases when ancient deposits are studied, for which it is hard to identify the initial composition of the metal-bearing solutions. In contrast to the representative materials on the composition of hydrothermal solutions and massive sulfide ores, data on the composition of material that precipitated near vents and

on its fluxes are very scarce, and only unsystematic data on some hydrothermal fields in the Pacific Ocean are now available from the literature [4–8].

This paper discusses the composition of the sedimentary material collected immediately beneath the smoke of black smokers in the Atlantic Ocean with the use of sediment traps in the course of the *BRAVEX/94* cruise [9]. The traps were fairly precisely deployed by *Mir* submersibles at a distance of 3 m from the bottoms of black smokers at two hydrothermal fields: TAG and Broken Spur. Both of the fields are underlain by basalts within the rift valley of the slow-spreading Mid-Atlantic Ridge (MAR). The material collected by a trap at the Broken Spur field was already partly described elsewhere [10, 11], whereas data on the composition of the hydrothermal–sedimentary material collected by a trap at the bottom of a black smoker at the TAG field have never been published before. The major difference between these fields is the age of their active edifices. The Broken Spur hydrothermal field is located within the axial zone of the rift valley and belongs to fields of the central type, along with the Squid Forest, Lucky Strike, Snake Pit, and Pui de Fol [12]. The 13 edifices (which are mostly active) discovered at the field contain approximately 100000. t of sulfide ores [13]. According to Bogdanov [14], they were accumulated for no more than 1 ka. The TAG hydrothermal field is related to a long-lived system that is spatially restricted to the marginal part of the rift valley. According to modern estimates, the active mound of the edifice contains ~2.7 mln. t of ore, and an additional 1.2 mln. t are contained in its roots [15], which penetrate into the basaltic basement to a depth of 125 m. Using isotopic dating techniques, Laloey et al. [16–18] demonstrated that the massive sulfide ores started to form there at 40–50 ka. The difference between the ages of the hydrothermal fields allowed us to reveal characteristic evolutionary differences in the mineralogy and chemistry of the collected hydrothermal–sedimentary material.

METHODS

Thanks to the simplicity of their design and convenience of exploitation, sediment traps are widely utilized in various types of studies. They enable the researcher not only to collect material deposited in a water column but also to assay the fluxes. An undoubted advantage of this method is the possibility of collecting amounts of material sufficient for detailed mineralogical and chemical study. Traps were used for examining the composition and fluxes of hydrothermal–sedimentary material practically immediately after the discovery of active hydrothermal springs [4, 6–8]. The studying of sedimentation processes within selected areas at hydrothermal fields with a high spatiotemporal variability of fluxes put forth the task of increasing the representativeness of the samples. The point is that the sampling cup of a trap rigidly connected to its cone bottom collects accompanying material when the trap is deployed and then lifted aboard, and it is then practically impossible to separate this material from that collected at a specified water level. To preclude this "contamination," the traps were equipped with devices that made it possible to isolate the sampling cups in the course of trap deployment and lifting. To study material fluxes at active hydrothermal fields, we designed and tested two KSL-400/1 sediment traps [19] equipped with devices for the isolation of the sampling cups to preclude the contamination of the material. The disadvantages of this technique are as follows. The trap preferably collects "heavy" material, which readily sinks in seawater, whereas fine particles usually remain in a suspended state in the water column due to the Brownian agitation of water molecules.

One KSL-400/I trap was deployed using a *Mir* submersible at the Broken Spur hydrothermal field at the bottom of the largest Saracen Head edifice. The fluid discharged from the head of this edifice had a temperature of 362°C. The position of the trap is schematically shown in Fig. 1. The area of the cone of the trap was 0.125 m^2. Over its exposure time of 17.5 days, the trap colleted 4.0 g of dry material. Table 1 presents a description of this material under a binocular microscope in water. Another trap was deployed in an analogous manner at the TAG field, near the top of a mound crowned with a black smoker in its upper part, at a distance of 3 m from the most massive chimney (Fig. 2). Over the exposure time of 5.87 days, the trap collected 3.87 g of dry material, whose description under a binocular microscope is presented in Table 2.

Processing of trap samples. Experience indicates that the processing strategy of material samples collected in a water column can fundamentally affect the results. Particular attention should thereby be paid to samples collected by sediment traps. Inasmuch as the granulometry and composition of this material are extremely diverse and heterogeneous, this material can be examined using a broad spectrum of methods and analytical techniques. Different sampling strategies sometimes led to differences in the results, which, in turn, initiated specialized studies with the aim of developing common approaches to sampling strategies, sample preparation, and the laboratory analysis of trap material. In processing the samples, we adhered to universally adopted recommendations [21].

During the preparatory stage (aboard), we assayed the collected material under a microscope (Tables 1 and 2) and separately identified biogenic and abiogenic particles. Biogenic particles were identified by S.V. Galkin and A.L. Vereshchaka (Shirshov Institute of Oceanology, Russian Academy of Sciences), and the preliminary description of the mineral components was conducted by A.Yu Lein (same institute). The sample was then held until the complete precipitation of the mineral constituent, and the remaining liquid with suspension was filtered through Whatman GF/FC glass

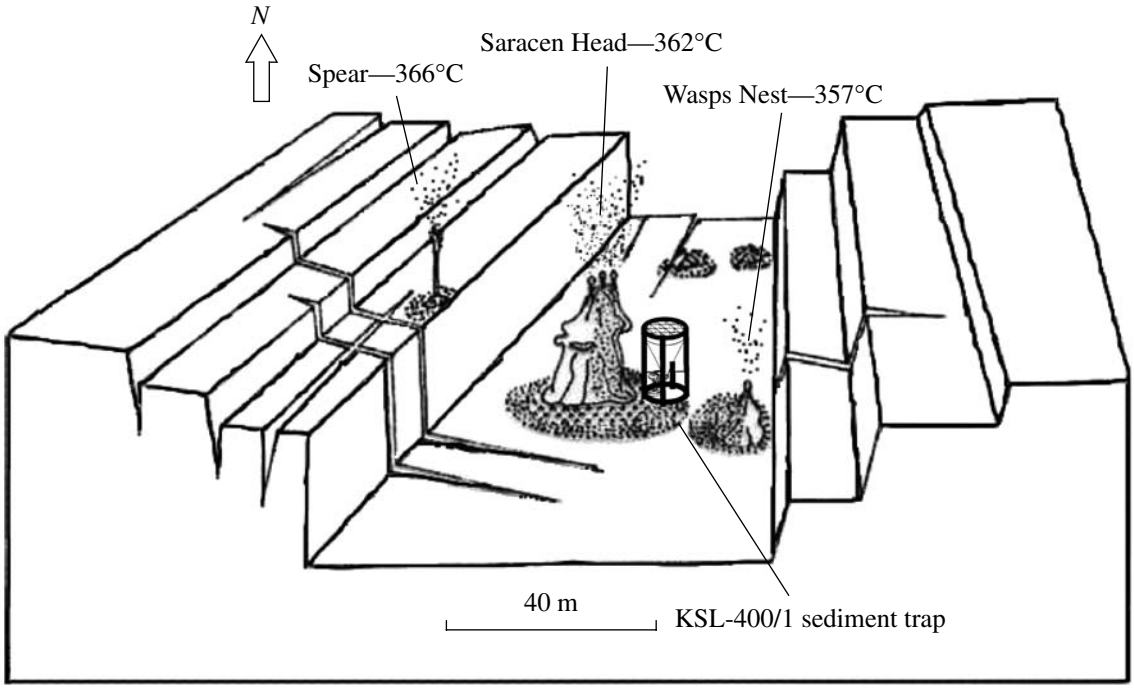

Fig. 1. Schematic cross section through the Broken Spur field [20] and the deployment site of the KSL-400/1 sediment trap. The trap is shown out of scale (enlarged).

fiber filters. The precipitate and filtered suspension were washed by twice distilled water to remove soluble salts. The material was then dried at a temperature of 55°C and hermetically packed to store for further analysis in the laboratory. A generalized treatment scheme of the samples is displayed in Fig. 3.

The chemical composition of the material was determined (only of its mineral constituent) by neutron activation (analyst D.Yu. Sapozhnikov, Vernadsky Institute of Geochemistry and Analytical Chemistry, Russian Academy of Sciences) and atomic adsorption (analyst L.L. Demina, Shirshov Institute of Oceanology, Russian Academy of Sciences). The results of analyses for organic carbon in the precipitated matter point to its very low concentrations (C_{org} = 0.15%) [10,11]. The bulk of C_{org} appeared to be contained in suspended matter (5–6%) (analyst L.V. Demina, Shirshov Institute of Oceanology, Russian Academy of Sciences). The results of chemical analyses are summarized in Table 3.

The granulometric composition was determined by conventional techniques at the Analytical Laboratory of the Shirshov Institute of Oceanology, Russian Academy of Sciences by V.P. Kozakova (Fig. 4). The mineral composition is presented based on the results of X-ray diffractometry on a DRON-4 analyzer (analyst V.V. Serova, Shirshov Institute of Oceanology, Russian Academy of Sciences). It was most difficult to deter-

Table 1. Material precipitating from the smoke of the black smoker at the Broken Spur field (collected by a sediment trap)

Composition, %	Organogenic material (~15%)	Mineral nonore material (~10%)	Mineral ore material (~75%)
Suspended matter (~15%)	Aggregates of organic detritus and sea (plankton) "snow" flakes	–	–
Precipitated material (~85%)	Fragments of shrimp carapaces; single foraminifer, gastropod, radiolarian, and pteropod shells; polyhaeta tubes and copepod carapaces	Anhydrite grains and aggregates, mica flakes, feldspars, quartz, and white nontransparent fragments of hydrothermally altered basalts	Flakes of pyrrhotite crystals, single pyrite and sphalerite crystals and aggregates (>0.1 mm), orange-brown aggregates of oxidized sulfides, and single chalcopyrite grains

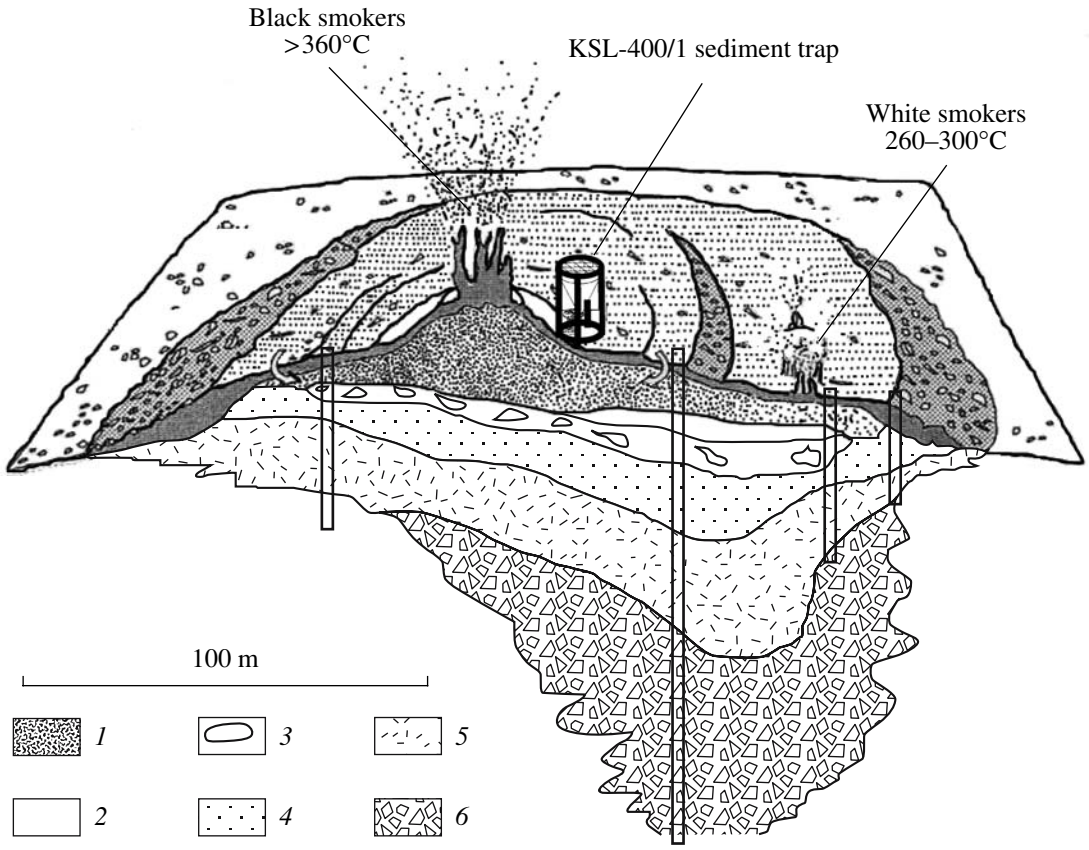

Fig. 2. Schematic cross section through the active TAG mound [15] and the deployment site of the KSL-400/1 sediment trap. The trap is shown out of scale (enlarged). (*1*) Massive pyrite breccia; (*2*) pyrite–anhydrite breccia; (*3*) pyrite–anhydrite–siliceous breccia; (*4*) pyrite– siliceous breccia; (*5*) basalt breccia cemented by amorphous silica; (*6*) basalt breccia.

mine the concentrations of Fe hydroxide species. Preliminary examination under a binocular microscope revealed its fairly high contents in the trap material from the TAG field, but Fe hydroxides do not yield X-ray diffraction patterns. Because of this, their concentrations were assayed visually in smear slides under a polarizing microscope (analyst A.A. Karpenko, Shirshov Institute of Oceanology, Russian Academy of Sciences). Based on these determinations, we semi-quantitatively assayed the mineral composition of the samples (Table 4). The mineral material was examined under a microscope in polished thin sections in reflected light that were prepared without heating, with preliminary saturation with epoxy resin. The microscopical studies were conducted by V.N. Apollonov (Institute of the Geology of Ore Deposits, Petrography, Mineralogy, and Geochemistry, Russian Academy of Sciences).

Table 2. Material precipitating from the smoke of the black smoker at the TAG field (collected by a sediment trap)

Composition, %	Organogenic material (~20%)	Mineral nonore material (~2%)	Mineral ore material (~78%)
Suspended matter (~10%)	Aggregates of organic detritus and sea (plankton) "snow" flakes	–	–
Precipitated material (~90%)	Fragments of shrimp carapaces; single foraminifer, radiolarian, gastropod, and pteropod shells; polyhaeta tubes and copepod carapaces	Anhydrite grains and aggregates, mica flakes, feldspars, quartz, and white nontransparent fragments of hydrothermally altered basalts	Aggregates of dark brown Fe hydroxides, sulfides covered with ocher, and aggregates of pyrite and sphalerite crystals

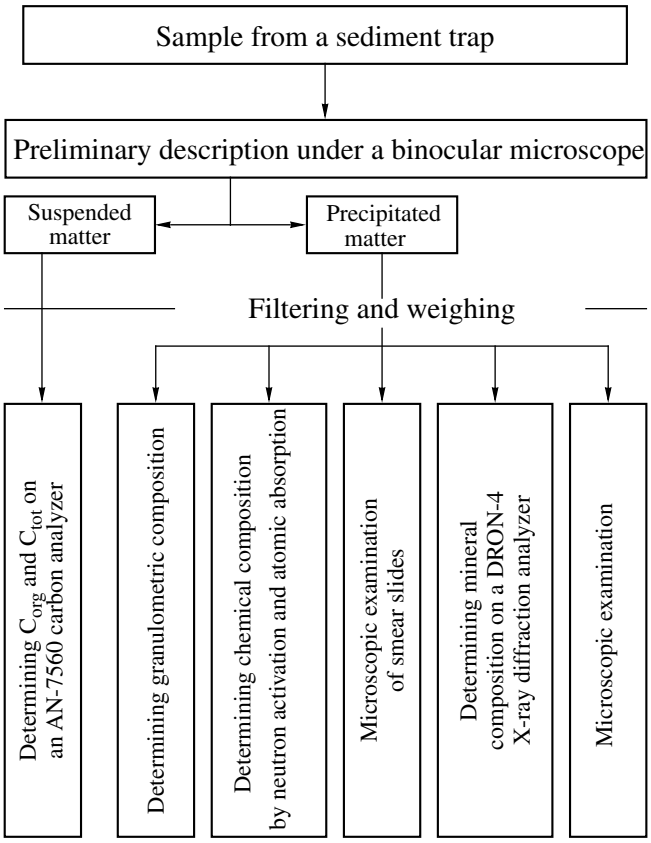

Fig. 3. Schematic chart of the processing routine of trap samples.

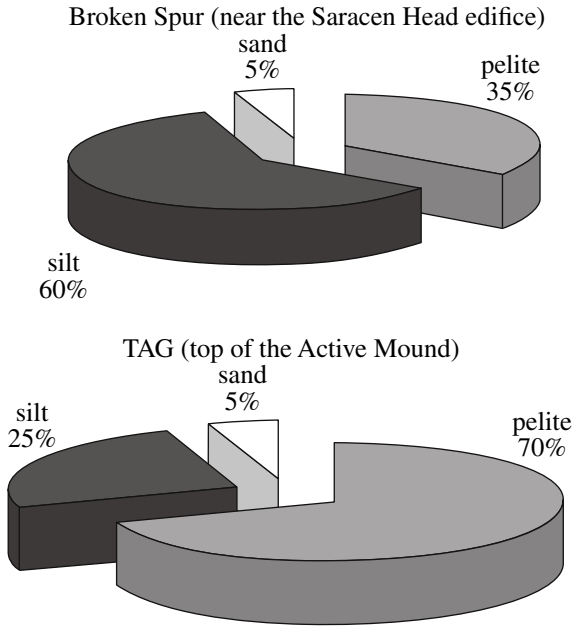

Fig. 4. Granulometric composition of trap material.

RESULTS

Saracen Head Edifice, Broken Spur Field

The **composition** of the trap material collected at a 3-m distance from the bottom of a black smoker chimney is dominated by sulfides in a silt granulometric fraction (~60%). The material consists mostly of lacy flakes of pyrrhotite aggregates (0.01–0.1 mm) with abundant pyrite, sphalerite, isocubanite, and chalcopyrite crystals and aggregates. Some of them are contained in the pelite fraction, which also includes fine powder of Fe oxi-hydroxides. The sand fraction (~5%) consists of massive sulfide grains: aggregates of isocubanite and anhydrite grains and aggregates of marcasite and pyrite (up to 3 mm across). The material sometimes contains large (up to 1 mm) corroded monocrystalline grains of anhydrite with pyrite inclusions. The material generally represents the composition of the zone where ore minerals rich in iron are actively deposited, along with minerals rich in calcium (anhydrite and hydrothermal calcite), and silicon (amorphous silica), barium (in barite), and aluminum (in aluminosilicates). The chemical and mineral composition of the collected material enabled us to calculate the contents of major components under the assumption that Fe is contained mostly in sulfides and hydroxides, Ba in barite, and Si in the form of amorphous SiO_2. To assay the fraction of organic matter (OM), we utilized the formula OM = $C_{org} \times 2$ [27]. The content of lithogenic material (LM) was calculated from the Al concentration and the average concentration of this element in the lithosphere (8.05%) [28]. The results of the calculations are presented in Fig. 5.

Mineral composition. According to their mineral composition, textures of mineral aggregates, and grain sizes, the trap material can be subdivided into five types (listed in order of decreasing frequency of occurrence):

(1) Flaky aggregates of thin-platy pyrrhotite (resembling snowflakes) with rare globules of pyrite and sphalerite (Figs. 6a–6d).

(2) Colloform–zonal textures (Figs. 6e–6h): (e) isocubanite–pyrite, (f) marcasite–pyrite, (g) marcasite–pyrite–sphalerite, (h) magnetite–sphalerite.

(3) Large, sometimes corroded monocrystalline grains of anhydrite, often with pyrite and chalcopyrite inclusions (Fig. 6i).

(4) Cubanite grains with pyrite rims (Fig. 6j).

(5) Dendrites (Figs. 6k, 6l): (k) pyrite, (l) sphalerite–marcasite.

Mineralogically, the trap material is dominated by pyrrhotite and pyrite, whereas the massive ores of the Saracen Head sulfide edifice consist mostly of pyrite, chalcopyrite, isocubanite, and sphalerite with an anhydrite admixture [29]. A composition similar to that of the trap material is characteristic of diffusers (beehive-shaped overgrowths on smoker chimneys). According to Butler and Nesbitt [30], the inner parts of diffuser channels are strongly dominated by pyrrhotite (50–90%), and

Table 3. Concentrations of chemical elements in the hydrothermal fluid of black smokers at the Broken Spur, TAG, and 21°N EPR fields and in the hydrothermal–sedimentary material collected by a sediment trap in the immediate vicinity of a spring

Parameter/Field, material	*T*, °C	pH	Cl	Ca	P	C_{org}	H_2S	Si	Ba	Fe	Cu	Zn	As	Ni	Co	Se	Sb	Al
		25°, 1 atm	g/kg				mg/kg											mg/kg
Broken Spur																		
Solution**	356–364	–	16.6	0.49	–	–	16.6	–	>2	110	2.8	4.7	–	–	–	–	–	–
Trap*	–	–	–	43	0.1	60	–	4600	370	371000	7000	7000	63.5	32	205	317.4	4.7	1100000
TAG																		
Solution***	360–366	<3–3.8	22.5	1.23	–	–	17–119	800	–	312	9.5	3.0	–	–	–	–	–	109
Trap*	–	–	–	32	2.2	50	–	24700	910	350000	10000	8500	191	102	379.6	77.6	8.9	1300000
21°N, EPR																		
Solution****	273–355	3.3–3.8	18.2	0.69	–	–	247	510	7.9	88	1.45	5.3	–	–	17	–	–	120
Seawater	1–5	7.8	19.3	0.4	–	–	0	2.1	0.2	<0.00006	0.00025	0.00065	–	–	2	–	–	1

Note: Data from * this publication, ** [20, 22], *** [23, 24], **** [25].

Table 4. Comparison of the mineral composition of material precipitated by the smoke of the Broken Spur and TAG fields (based on X-ray powder diffraction data, analyst V.V. Serova, Shirshov Institute of Oceanology, Russian Academy of Sciences) and the field at 21°N, East Pacific Rise (EPR) [7, 26]

Mineral	Idealized formula	Broken Spur	TAG	21°N, EPR
Pyrrhotite	$Fe_{1-x}S$	+++++	++	++++
Pyrite	FeS_2	++++	++++	+++++
Sphalerite	ZnS	+++	+++	+++++
Chalcopyrite	$CuFeS_2$	++	+++	++
Fe oxi-hydroxides		+	+++++	++
Calcite	$CaCO_3$	+	+	?
Opal	$SiO_2 \cdot nH_2O$	+	++	++
Anhydrite	$CaSO_4$	+++	+++	++
Barite	$BaSO_4$	+	+	+
Wurtzite	ZnS	–	++	++
Isocubanite	$CuFe_2S_3$	++	++	++
Marcasite	FeS_2	+	+	+

Note: Abundances: +++++ very much, ++++ much, +++ moderate amounts, +++ little, + traces, – not found.

their outer parts consist mostly of pyrite, marcasite, and sphalerite. The aggregates of the edifice and the particles collected by sediment traps also show certain structural differences. For example, aggregates of thin platy pyrrhotite and colloform–zonal aggregates of grains from the edifice are more massive and coarser grained. The zonal structures and textures of the ores of the edifice definitely testify to the recrystallization of material during the growth of this edifice [31]. In the trap material, the zonal textures of particles, conversely, exclusively reflect the variations in the thermochemical conditions of the mineral-forming processes during the growth of the particles in the course of their ascent along the fluid feeders of the edifice. There are obviously two simultaneous mechanisms of ore deposition: the growth of massive ores by precipitation from fluid on the inner walls of the fluid channels with associated metasomatic replacements and the deposition of material (as a result of volumetric precipitation from oversaturated solutions) immediately in the flow of hydrothermal solutions at variations in the thermochemical parameters. The latter processes produces the fine particles of the smoke of black smokers.

Fluxes. Proceeding the exposure times of the traps, the amount of collected material, and the areas of the collection cones, one can easily calculate the fluxes of sedimentary material and its discrete components. As can be seen from Fig. 7, the structure of the flux is dominated by Fe sulfide species. The second most abundant chemical element in the flux is Ca, which forms mostly sulfates. It was determined that the source of Ca^{2+} is hydrothermal solutions, whereas SO_4^{2-} is borrowed from seawater [32]. Thus, anhydrite is formed with the participation of seawater. Under oxidizing conditions (in seawater), Ca sulfates and Fe oxi-hydroxides are formed. Our samples also contained single crystals of aragonite, which is formed in the low-temperature part of the hydrothermal plume immediately above the vent.

The extensive studies of plankton communities inhabiting the Broken Spur field [33] have revealed high plankton contents: from 1 mg/m^3 at 1 km from the vent to >600 mg/m^3 within a few meters from it. In the immediate vicinity of the smoker, shrimp "clouds" were detected, which fed mostly on chemosynthetic bacteria. Their remnant maintain an elevated OM flux in the zone of the active precipitation of ore minerals (Tables 1, 2).

The flux of amorphous silica is less significant. It was calculated from the Si concentration in the samples. However, according to data obtained at a vent in the active field of the Juan de Fuca Ridge [4, 5], some silica amount can be spent on Fe–S–Si phases that are hard to identify by X-ray diffraction. At the same time, the simulation of geochemical mineral-forming processes [34] indicates that the drastic cooling of hydrothermal solutions leads to the crystallization of a phase consisting of 30–70% amorphous silica. The high silica concentrations in the hydrothermal solution and contrastingly low contents in the trap material possibly suggest that Si forms very fine-grained suspended material that is disseminated by flows and does not sink to the seafloor. According to other data [32], much silica does not form any mineral phases but is supplied to seawater in the form of solution.

TAG Field: The Top of the Active TAG Mound

Chemical and mineral composition. The trap material is characterized by high concentrations of Fe-bearing minerals in the form of sulfides and hydroxides (Table 4). Compared to the material from the trap at the Broken Spur field, this material is dominated by Fe oxi-hydroxides (41%) and has somewhat elevated contents of amorphous silica (Fig. 5). The predominant sulfide is pyrite, and the material contains low concentrations of chalcopyrite. It should be mentioned that the trap material contains much less pyrrhotite than the material from the Broken Spur field, and this mineral is absent from the edifice [35–37]. It is reasonable to suggest that the growth of the edifice was associated with complete pyrrhotite replacement by pyrite or marcasite.

The mineral composition of the massive ore of black smokers at the TAG edifice is similar to that of the Saracen Head edifice: anhydrite–chalcopyrite–silica with notable amounts of marcasite [29, 35, 36]. Edifices resembling Kremlin towers (white smokers) at a distance of 70 m from the black smokers differ from the

latter in having lower temperatures and higher Zn concentrations of the discharged solutions. High concentrations of Fe and Mn oxi-hydroxides were detected only near the bottom of the ore edifice [36].

We also posses unique data on the inner structure of the orebody and the material beneath it [15]. These data were obtained via deep drilling (Fig. 2). The edifice rests on breccias of hydrothermally altered (to the greenschist metamorphic facies) basalts cut by quartz–pyrite stockworks (roots of the edifice). The peripheral zone of the roots is characterized by strong chloritization of basalts. The upper part of the subore material contains basalt breccia cemented by amorphous silica. The roof of the orebody is dominated by sulfide ore minerals, predominantly pyrite. The central part of the edifice is made up (like many samples) mostly of anhydrite with pyrite and chalcopyrite inclusions. The general inner structure of the orebody and its host rocks made it possible to ascribe it to deposits of the Cyprian type [38].

Fluxes. In the zone of active sulfide precipitation, the total flux of sedimentary material equals 5200 mg/m^2/day (Fig. 7), which is 2.8 times higher than the total flux at the vent of the Broken Spur field and is hundreds of times higher than the fluxes outside hydrothermal fields [39]. The predominant chemical element of the flux is Fe (1820 mg/m^2/day) in the form of hydroxide and sulfide minerals. The total flux of the latter is close to 3500 mg/m^2/day. Relatively high fluxes are also typical of Zn and Cu: 44 and 52 mg/m^2/day, respectively. These elements occur mostly in the form of sulfides (sphalerite, wurtzite, and chalcopyrite), and their total flux amounts to 150 mg/m^2/day. Other significant fluxes are those of amorphous silica (274 mg/m^2/day) and authigenic Ca carbonates and sulfates (aggregate flux of 187 mg/m^2/day). In spite of the very high fluxes of sedimentary material in the active deposition zone of ore minerals, much of the material is removed by bottom currents outside the hydrothermal field. Comparing the amount of Fe introduced by springs at the TAG field (which was estimated to 2200 t/yr [40]) with our evaluations of its precipitation (no more than 2.3 t/yr [39]), it can be seen that the amount of Fe hydrothermally precipitated within the ore field is 1000 times (!) lower than the amount of introduced Fe. This also fully pertains to Si, Ca, and Ba, which are mostly scattered and disseminated in the form of solutions or suspended matter in the water masses and lose their relations with the spring. Furthermore, we determined [41] that the plume above the TAG field 6 km^3 in volume contains approximately 67 t of Fe in the form of suspended matter, and the plume above the Broken Spur field 8.24 km^3 in volume contains as little as 23.5 t of Fe. This confirms a high influx of Fe oxi-hydroxides in the form of fine suspensions, which are contained in the hydrothermal plume above the TAG field.

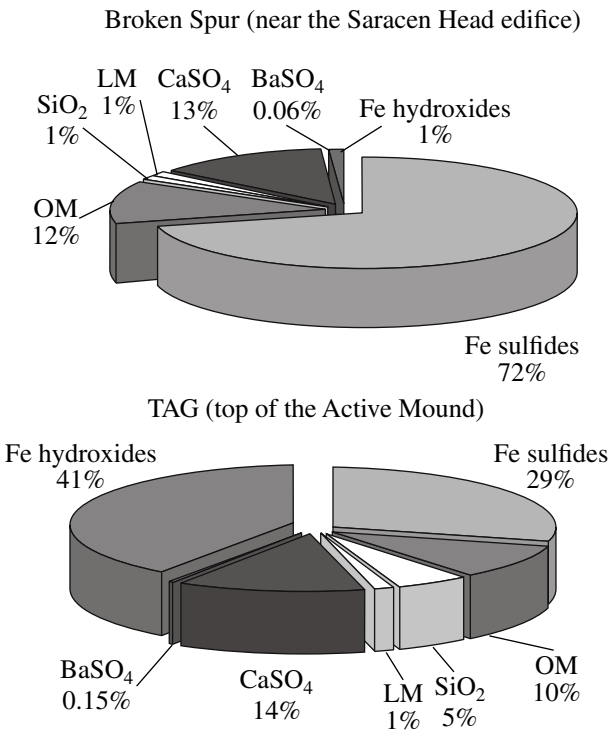

Fig. 5. Composition of trap material (see text for symbol explanations).

DISCUSSION

Formation of the hydrothermal–sedimentary material. Studies at various submarine hydrothermal fields have revealed certain zoning in the formation of the hydrothermal–sedimentary material. In its general form, this zoning is controlled by the degree of mixing of the high-temperature mineralized fluid and cold seawater. According to the model research conducted by Janecky and Shanks [42], oversaturated solutions under conditions close to the state of a hydrothermal fluid (~350°C, seawater/fluid ~1/10) precipitate Cu sulfides: chalcopyrite and bornite. Magnetite and pyrite are also formed under similar conditions and correspond to the composition of the vertical chimneys of black smokers. The final, low-temperature member of this succession (at fluid strongly diluted by seawater: seawater/fluid > 1/10) is sphalerite, a sulfide most typical of white smokers. Other minerals actively precipitating under similar conditions, along with sulfides, are high-temperature anhydrite, whose crystallization temperature is higher than 130°C [26]. The reason for its crystallization is elevated SO_4^{2-} concentrations in seawater. The wide occurrence of anhydrite among the mineral assemblages of the TAG edifice testifies to the active penetration of seawater into the orebody and its contact with the hydrothermal fluids. The next minerals precipitating as suspended matter are amorphous silica, which is the most typical constituent of the subore material, and Ba sulfate (barite). In oxidizing environments (sea-

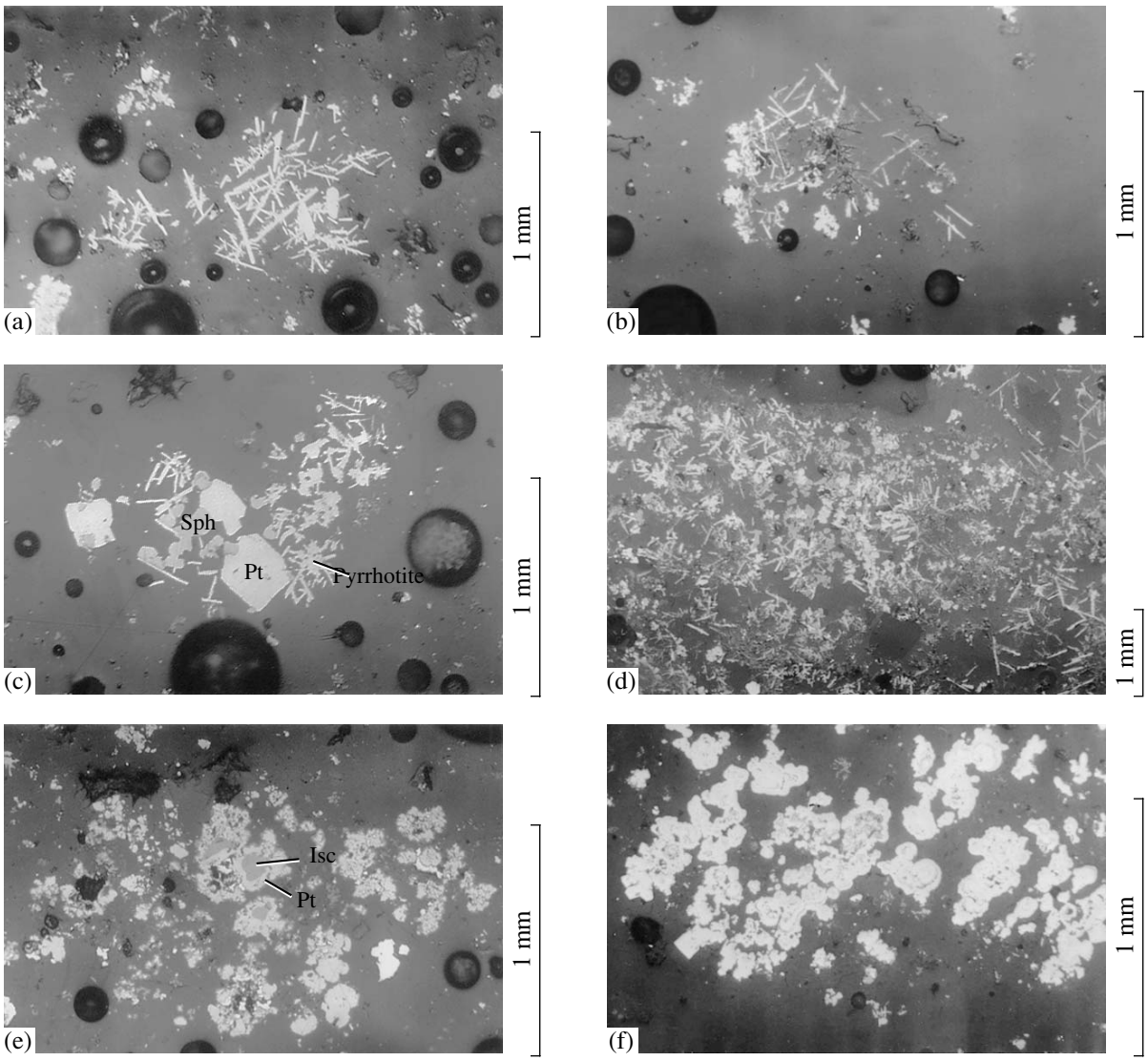

Fig. 6. Trap material (Broken Spur field) in thin section. Black globules are air bubbles. (a–d) Flakes of pyrrhotite aggregates with single (c) pyrite and sphalerite grains; (e–h) colloform textures of (e) isocubanite–pyrite, (f) marcasite–pyrite, (g) marcasite–pyrite–sphalerite, and (h) magnetite–sphalerite composition; (i) corroded single crystal of anhydrite with inclusions of tiny pyrite and chalcopyrite grains; (j) isocubanite grain with a pyrite rim; (k, l) dendrites of (k) pyrrhotite and (l) sphalerite–marcasite composition.

water), Fe forms individual oxides and hydroxides: magnetite ($FeFe_2O_4$), hematite (Fe_2O_3), goethite ($HFeO_2$), lepidocrocite (FeOOH), and hydrogoethite ($HFeO_2 \cdot nH_2O$). The processes forming sulfide and sulfate minerals practically terminate when the temperature falls to the ambient seawater temperature (approximately 2°C). Observation data at the TAG field [43] indicate that the temperature anomaly for an ascending plume at a height of 50 m above the vent reaches 0.2°C, i.e., is virtually equal to the ambient water temperature, and the dilution coefficient is >500. By that time, part of the Fe^{2+} ions of the primary metalliferous solution is accommodated in sulfide minerals. The same time span is characterized by the crystallization of Cu, Zn, and Pb sulfides and the precipitation of elementary S particles. During the further ascent of the plume (its oxidizing part), the remaining Fe^{2+} ions produce Fe^{3+} oxi-hydroxides. This process ends at a height of about 120 m above the vent (at >2000 dilution of the hydrothermal fluid by seawater). Thus, the processes forming the bulk of hydrothermal minerals are practically ceased already in the ascending plume zone. The precipitation succession of ore minerals into particulate matter can be as follows: chalcopyrite—isocubanite—pyrite (marcasite)—magnetite—sphalerite—Fe hydroxides. The succession for nonore minerals is anhydrite—amorphous silica—barite.

It is commonly thought that the deposition of the hydrothermal–sedimentary material is spatially restricted to the vent of a spring (ascending plume),

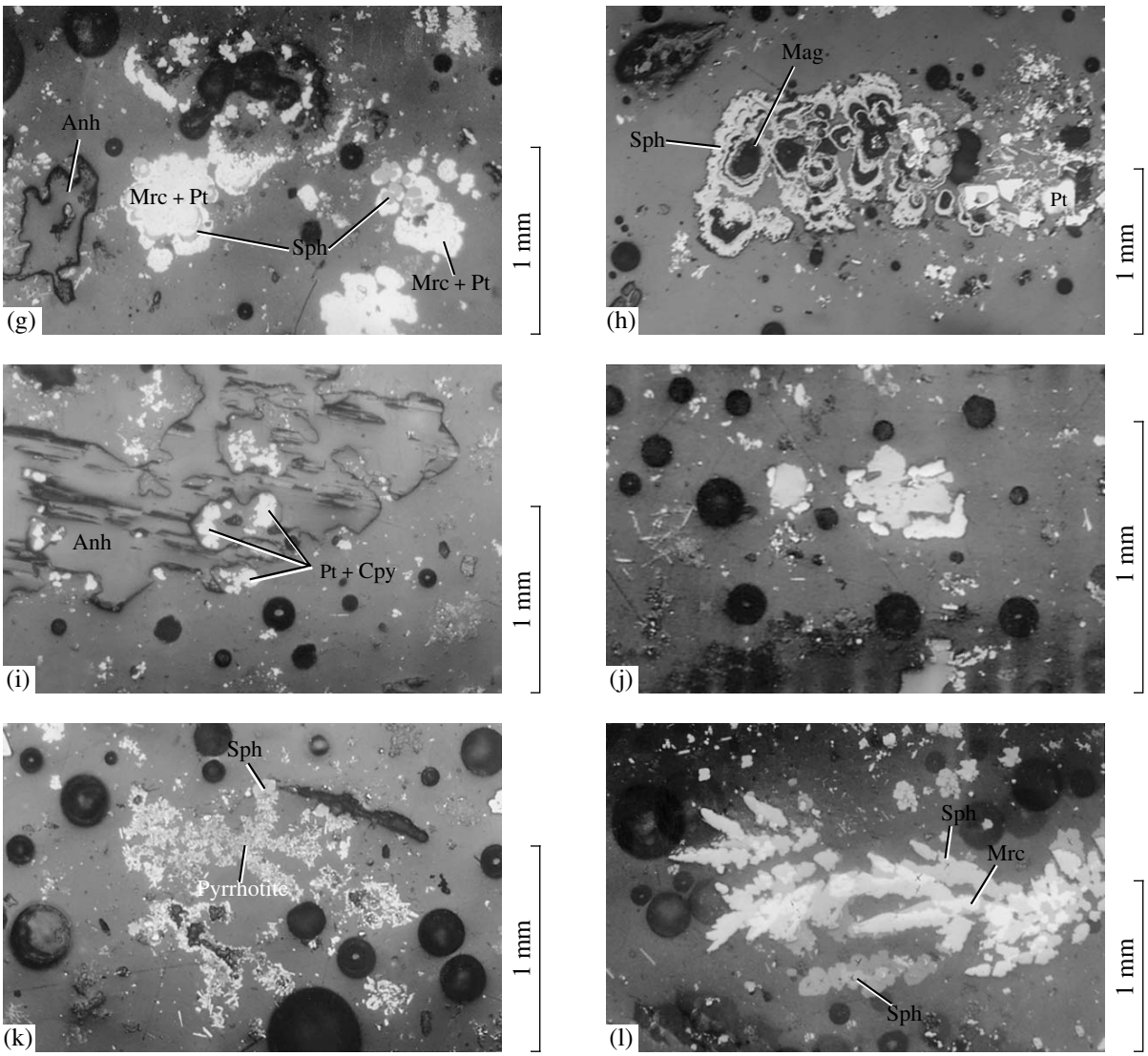

Fig. 6. Contd.

where the temperature and geochemical gradients are at a maximum. However, detailed research of the mineral composition of the trap material has revealed that part of this material (its highest temperature minerals) start to precipitate already within the fluid conduits, i.e., before the hydrothermal solution reaches the vent of the black smoker. It is believed that solutions can form minerals in at least two manners: by the direct crystallization due to oversaturation and via precipitation in response to a drastic change in the physicochemical parameters of the environmental equilibrium. In the former situation, a limited number of crystallization centers is produced, and consequently, relatively large mineral crystals can grow. In the latter instance, numerous crystallization centers (whose concentration in a given volume increases with increasing oversaturation of the solution) produce cryptocrystalline material, which resembles colloid; and, finally, colloids themselves can be generated if the degree of oversaturation is particularly high. Colloids are known to be heterogeneous two-phase systems (dispersion medium + dispersed phase). By analogy with Au and Ag solutions, Fe colloid solutions can be attributed to the group of liophobic colloids, which are heterogeneous and unequilibrated systems [44]. High concentrations of a dispersed phase create favorable conditions for the spontaneous coagulation of colloid particles with the development of globular aggregates with colloform textures. The onset of noticeable coagulation requires the electrolyte concentration to be higher than a certain limit, which can be readily reached by an increase of the seawater fraction in the solution (sensibilization). However, the problem of the early stages of the origin of micelles remains unsettled as of yet.

Colloform textures were often described at sulfide ore deposits, and relics of these textures are sometimes

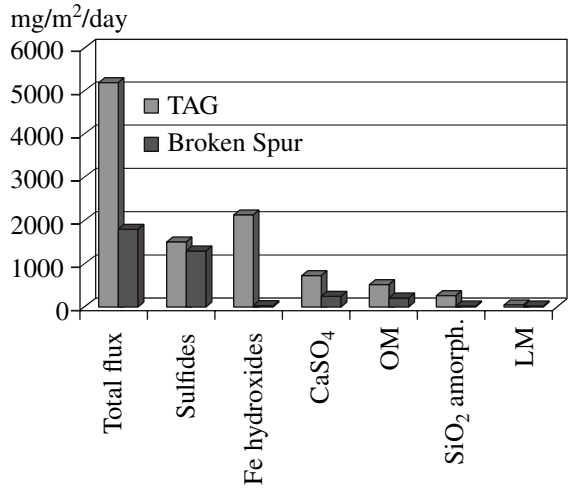

Fig. 7. Fluxes of hydrothermal–sedimentary material and its components at a distance of 3 m from the Saracen Head edifice, Broken Spur field, and black smokers at the top of the TAG Active Mound (see text for symbol explanations).

spread so broadly that they were thought to be related to hydrothermal ores. Betekhtin et al. [45] were the first to hypothesize that colloids may play a leading role in the genesis of these textures. These researchers have demonstrated that much of currently known sulfide ores were formed by oversaturated colloid solutions in response to a sharp change in the physicochemical parameters of the environment. It should be emphasized that relations between submarine hydrothermal systems and the deposition of sulfide ores was established only half a century later. It is also pertinent to mention that colloids can be produced within broad ranges of temperatures, pressures, and other conditions [44]. They are often formed in the course of low-temperature processes and produce colloform–zonal textures. These textures can also be formed by recrystallization during hydrothermal metasomatism. For example, colloform textures of chalcopyrite with rims of fine-grained sulfides in hydrothermal sulfide ores are generated by the transformation of the crystal structure of Cu sulfide at deviations from the stoichiometry in the Cu–S system [46]. A metasomatic mechanism forming colloform textures was also determined for zonal–rhythmical chalcopyrite–sphalerite spherulitic aggregates [29]. The latter are, however, the most ubiquitous in mature edifices, which are characterized by widespread multistage exsolution textures of solid solutions within a broad temperature range. Colloform textures of metasomatic genesis can be readily distinguished from hydrothermal–sedimentary particles because of the less massive and finer grained textures of the latter.

Taking into account the precipitation succession of minerals in the form of particulate matter in the course of fluid mixing with seawater and a decrease in the solution temperature, the colloform mineral aggregates collected by our trap (Figs. 6e–6h) can be arranged in the following sequence: isocubanite–pyrite, pyrite–marcasite, pyrite–marcasite–sphalerite, and magnetite–sphalerite. According to laws of colloid chemistry, the core of a globular aggregate (micelle) formed by coagulation is not necessarily made up of the compounds precipitated earlier from the solution, but instead the determining factor is the concentrations of the dispersed phase of a certain mineral. The higher this concentration, the higher the probability of its coagulation. The onset of the crystallization of colloform rhythmically zoned magnetite–sphalerite aggregates (Fig. 6h) was undoubtedly triggered by the precipitation of minute magnetite grains. The growth of magnetite particles depleted the dispersed phase in this mineral and, as a consequence, led to a change of the coagulant. The particle continued to grow via the precipitation of sphalerite. It is interesting to note that some grains contain three and occasionally even more magnetite–sphalerite rhythms. Coagulation and subsequent sorption occur very selectively and form only some mineral assemblages, obviously because of the electrokinetic characteristics of the dispersed system.

At the same time, colloid solutions do not necessarily produce colloform textures. At a low concentration of the dispersed phase and high enough contents of necessary components in the solution, *holocrystalline textures* can be formed, such as aggregates of sulfide minerals. Dispersed particles consisting of crystalline compounds carry an electric charge at the edges and vertices of crystals. The resultant residual uncompensated charge facilitates the adsorption of certain ions from the solution.

For metal and sulfur ions to interact, the solution should contain a certain concentration of dissociated molecules. Dissolved H_2S is thought to be able to decompose chloride complexes (which contain the bulk of metal in fluids), i.e., Fe polysulfides can be formed under reducing conditions according to the reaction

$$FeCl_2 + H_2S_n = FeS_n + 2H^+ + 2Cl^-. \quad (1)$$

However, as follows from the results of laboratory experiments [47], H_2S_n polysulfides can be formed via the partial oxidation of H_2S or HS^- when hydrothermal solutions interact with seawater according to the reaction

$$nH_2S\ (aq) + (n-1)/2O_2 = H_2S_n + (n-1)H_2O. \quad (2)$$

At temperatures below 250°C, acidic solutions with pH 5 precipitate marcasite along with pyrite or instead of it by the reaction

$$Fe^{2+} + H_2S_n = FeS_2 + S^0_{n-2} + 2H^+. \quad (3)$$

This mechanism likely produces pyrrhotite crystals that subsequently precipitate as particulate matter upon the outflow of solutions from the vent of the smoker, according to the reaction

$$Fe^{2+} + H_2S = Fe_{(1-x)}S + 2H^+. \quad (4)$$

A no less interesting issue is the genesis of **dendrites**. Although they are relatively innumerous, they compose an independent group and have characteristic mineral assemblages. As is known, mineral aggregates of this type are formed by the rapid crystallization in thin cracks or in viscous liquids, i.e., when crystal growth is hampered by external conditions. The reasons for the development of these aggregates are still not fully understood. On the one hand, oriented crystal growth can be caused by the effect of a laminar fluid flow along fluid conduits. Conceivably, these aggregates could also originally develop in cracks in another mineral aggregate, which was later decomposed. An example is the widely known sphalerite dendrites in tiny cracks in the edifice at 14°45′N at MAR. They are often replaced by chalcopyrite as a secondary mineral [48].

The facts and considerations presented above led us to the following preliminary conclusions about the mechanisms forming the hydrothermal–sedimentary material. First, the simultaneous occurrence of holocrystalline and colloform aggregates in the trap material suggests their close spatiotemporal relations and provides evidence of the roughly simultaneous precipitation from both weakly oversaturated and strongly oversaturated (colloid) solutions. Second, the rhythmically zonal inner texture of the colloform aggregates testifies to numerous changes in the thermochemical conditions, perhaps as a consequence of the periodical oversaturation of the solutions during their ascent along channels in the edifice. Third, there obviously are two simultaneously acting mineral-forming mechanisms: direct precipitation from solutions and sorption–adsorption processes on the surface of earlier minerals.

Sources of chemical elements. Another important problem is the source of chemical elements during the formation of the hydrothermal–sedimentary material (hydrothermal solution or seawater). A principal indicator of the participation of a given element is its enrichment coefficient (EC) of the hydrothermal–sedimentary material relative to the composition of the primary metalliferous fluid. Considering the fact that Fe of the hydrothermal–sedimentary material is provided mostly by hydrothermal fluids, it is convenient to examine the concentrations of other chemical elements relative to the concentration of Fe (Table 5). As can be seen in Fig. 8, all elements can be provisionally subdivided into three groups. The first of them (log EC > 0) includes elements partly borrowed from seawater, the second group (log EC ~ 0) comprises elements whose concentrations do not increase relative to those in the hydrothermal solution, and the third group (log EC < 0) consists of elements whose concentrations decrease relative to those in the hydrothermal solution (Si, Ca, Mn, and Ba). The relative concentrations of ore elements (Co, Cu, and Zn) are close to those in the primary metalliferous solution, a fact testifying that these elements effectively precipitate as suspended matter and actively participate in the generation of the hydrothermal–sedimentary material. The main source of these elements is hydrothermal fluid.

Table 5. Enrichment coefficients (relative to the metalliferous fluids) of chemical elements in trap material collected beneath the smoke of black smokers at the Broken Spur (BS) and TAG fields. The coefficients were calculated by the formula EC = (Element/Fe) in trap/(Element/Fe) in fluid

Chemical element	Enrichment coefficient (EC)	
	BS	TAG
Cu	0.72	0.93
Zn	0.43	2.66
Al	–	8.59×10^{-4}
Ba	0.05	–
Ca	0.025	0.023
Si	–	0.027

The behavior of Al differs from those of other elements. The Al/Fe ratio in the solutions (3.49) is notably higher than in the trap material (0.003) (Table 6). At the same time, the higher relative Al contents in the suspended matter suggest its sorption on Fe oxi-hydroxides in the ascending plume and the resuspension of the fine material of the upper sediment layer by ascending hydrothermal flows. The analysis of the distributions of the ^{234}Th and ^{230}Th isotopes in the water column near the TAG vent [49] has demonstrated that particles 1–10 μm can be involved in recycling. However, our estimates [11] indicate that the "contamination" of the trap samples with re-suspended material does not exceed a few percent.

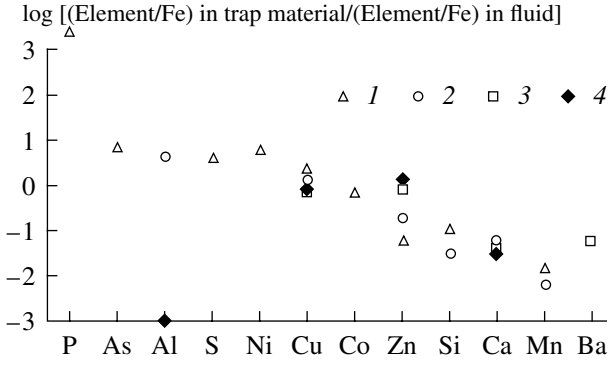

Fig. 8. Element diagram for trap material from the TAG and Broken Spur hydrothermal fields (element concentrations are normalized to their contents in the hydrothermal fluid). Suspended matter from springs at: (*1*) Juan de Fuca and (*2*) MAR [5]. Trap material from fields: (*3*) TAG; (*4*) Broken Spur.

Table 6. Elemental ratios in hydrothermal solution and sedimentary material collected in sediment traps at deployed black smokers within the Broken Spur and TAG fields. Data on the field at 21°N, EPR, are compiled from [25]

Element/Fe	Cu/Fe	Zn/Fe	Ca/Fe	Si/Fe	Se/Fe	As/Fe	Al/Fe
Material of	mg/mg				μg/mg		
Broken Spur							
Solution	0.025	0.042	4.45	–	–	–	–
Trap	0.018	0.018	0.11	0.01	0.85	0.17	0.003
TAG							
Solution	0.030	0.009	3.94	2.56	–	–	3.49
Trap	0.028	0.024	0.09	0.07	0.22	0.54	0.003
21°N, EPR							
Solution	0.016	0.06	7.84	5.79	–	–	0.001

Effect of metasomatic processes in the edifice on the composition of hydrothermal–sedimentary material. Detailed studies of the mineral associations of hydrothermal edifices revealed that the growth of these edifices is associated with continuous metasomatic transformations [50]. Pyrrhotite and sphalerite are replaced by pyrite. It was also noted that pyrite can replace other sulfides and even sulfates. The process of the replacement of minerals by pyrite at terrestrial sulfide deposits is thoroughly described in the literature and is extremely widespread. Its traces were first identified in hematite and magnetite ores in Ural (Kutumskoe deposit). According to [45], the process was initiated by an increase in the H_2S concentration in the metalliferous solutions during a certain deposition stage of ore minerals. The process obviously proceeded according to the reaction

$$2Fe_2O_3 + 2H_2S = Fe_3O_4 + FeS_2 + 2H_2O. \quad (5)$$

In some samples, pyrite replaced not only oxides but also silicates, when the latter interacted with S-bearing solutions. This process was usually associated with the introduction of S and removal of Fe (or Zn). For example, the elevated Zn and Au concentrations in ores from the zone of white smokers are explained by the remobilization of these elements from previously deposited sulfides of the edifice [15]. A good example of this is the metasomatic replacement of pyrrhotite by Fe disulfide (pyrite or marcasite) with the removal of Fe^{2+} from its crystal structure by the reaction

$$Fe_{(1-x)}S + S \longrightarrow FeS_2 + Fe^{2+}. \quad (6)$$

The ores often show evidence of the subsequent replacement of sphalerite by chalcopyrite and, then, bornite ($ZnS–CuFeS_2–Cu_2FeS_4$) according to reactions like

$$ZnS + S + Fe^{3+} + Cu^+ = CuFeS_2 + Zn^{2+}, \quad (7)$$

$$CuFeS_2 + 2S + Cu^+ = Cu_2FeS_4. \quad (8)$$

The detailed studies of Cu-bearing minerals in the Cu–Fe–S system at the Logachev and Rainbow fields [46] demonstrate that the Cu concentration in the orebody increases and Fe^{2+} is removed in an oxidizing environment under the effect of seawater: $Cu^+Fe^{2+}Fe^{3+}S_3$ (isocubanite)—$Cu^+Fe^{3+}S_2$ (chalcopyrite)—$Cu_5^+Fe^{3+}S_4$ (bornite).

At the same time, it cannot be ruled out that the predominance of Fe oxi-hydroxide species over sulfides in the trap material from the TAG field resulted from the deficit of sulfide sulfur in the solutions themselves. According to Grichuk's thermodynamic model [1], during the early circulation of solutions through "fresh" basalts, ore elements can be arranged in the following succession according to their relative mobility (defined as the ratio of the concentration of a given element in solution to the concentration of this element in fresh basalt): Pb > S > Zn ≈ Fe > Cu. This means that Pb is more rapidly removed from rocks than S and Zn, and Fe and Cu are leached more slowly. With increasing "age" of the recycling hydrothermal system, which is defined as the number of water portions that have passed through the rock, the relative concentrations of these elements change from S > Fe and Zn > Cu in a young system to Fe > S and Cu > Zn in a more mature one. This clearly demonstrates that the initial metalliferous solutions should become deficient in S during a certain evolutionary stage of the system. Hence, excess Fe should be inevitably incorporated not into sulfides but hydroxide during later stages.

Role of hydrothermal–sedimentary material in the development of the orebody. According to the character of sulfide ore mineralization, Smirnov [3] distinguished three classes of mineral deposits: volcanic–sedimentary, volcanic–metasomatic, and combined. The latter class of deposits is formed in at least two stages: the early hydrothermal–sedimentary submarine deposition of ore material and later overprinted hydrothermal–metasomatic processes. Proceeding from the age of a given hydrothermal field, the mass of material concentrated in the edifice, and the fluxes of sedimentary material from the smoke of the spring, one can assay the contribution of the hydrothermal–sedimentary material to the overall balance of ore material. The rate of ore material accumulation at the Broken Spur field is currently evaluated at approximately 100 t/yr [13]. With regard for the cyclicity of hydrothermal activity, the growth rate of the TAG edifice is roughly twice higher: close to 200 t/yr [14]. Our estimates obtained with the use of sediment traps indicate that the amount of hydrothermal–sedimentary material annually accumulated near the Saracen Head vent at the

Broken Spur field is close to 2 t, and the analogous value for the TAG edifice is approximately 6 t/yr. Thus, the ore material precipitating from the smoke is a little bit higher than 3% of the material of the edifices themselves. This means that the fields in question can be classed with typical deposits of the volcanic–metasomatic type, which are characterized by a strongly subordinate amount of sedimentary material.

Composition of the hydrothermal–sedimentary material and cycles of the hydrothermal process. The isotopic composition of the hydrothermal edifice [16, 17, 18] and metalliferous sediments [29] of the TAG field makes it possible to identify discrete cycles in the evolution of the hydrothermal ore-forming process. Over the past 26 ka, hydrothermal activity at the field has diminished three times and then increased again. Periods of hydrothermal activity lasted from 3–6 ka and gave way to periods of volcanic activity, which lasted 6–8 ka. The latter were identified by high contents of volcanic glass in the sediments. It was also noted that hydrothermal activity was synchronous at various vents of the TAG hydrothermal field. The last cycle, which lasted approximately 10 ka, included two activation peaks of springs at the Active TAG mound (Fig. 9), which were identified by the enrichment of the sediments in minerals produced by the presence of minerals of greenschist-facies alterations of basalts (chlorite, colorless mica, epidote, and clinozoisite). Their grains are 2–3 mm across and larger and suggest high rates of fluid inflow from the spring and the high fracturing of the basement. The attenuation of the hydrothermal activity was associated with an increase in the percentage of low-temperature material in the sediments. According to Lisitsyn [51], hydrothermal activity ends with the development of films and crusts of Fe and Mn oxi-hydroxides on the surface of the edifice. Bogdanov [29] and Gurvich [32] believe that hydrothermal activity at the TAG field reached its closing phase. Activity at the Mir hydrothermal edifice at the same field has already ceased (at ~700 ka) [18].

Unfortunately, modern deposits are absent from the stratigraphic columns, because the uppermost few centimeters of the sediments are lost in the course of sampling by ground corers. This gap in information can, however, be partly bridged by data obtained by sediment traps. For example, low contents of altered basalt fragments (~2%) in the trap material from the TAG field (Table 2) likely testify to a current relative decline in the hydrothermal activity of this field. At the same time, the content of these fragments in the material from the young Broken Spur field amounts to 10% (Table 1). This can be explained by the gradual clogging of minor fluid conduits with hydrothermal material and the focusing of the fluid discharge. The much higher overall flux of sedimentary material at the central spring of the Active TAG mound is obviously controlled by the higher outflow rate of the only remaining high-temperature vent at this field. Thus, the contents of fragments of metamorphosed basalts in the sedimentary material

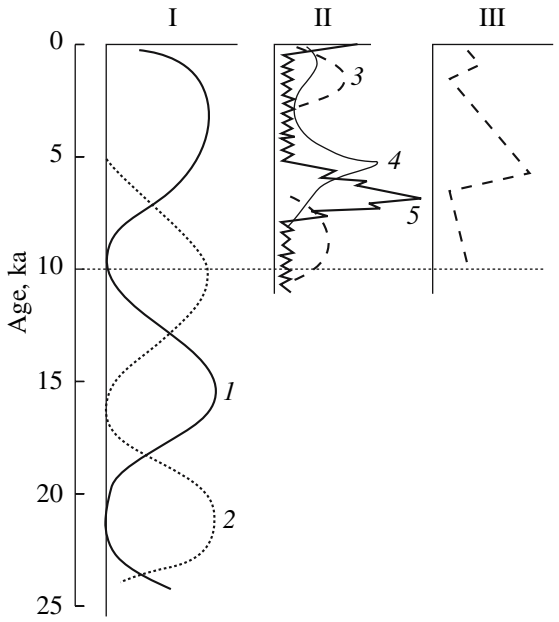

Fig. 9. Cyclicity of hydrothermal activity at the Active TAG mound reconstructed based on studying columns of bottom sediments (modified after [29, 32, 51]). (I) Cyclicity of (*1*) hydrothermal activity; (*2*) volcanic activity; (II) contents of hydrothermal component (relative units) in sediments: (*3*) Mn globules and crust fragments; (*4*) minerals of greenschist metamorphic facies; (*5*) Fe contents in bottom sediments; (III) outflow rate of hydrothermal solutions.

can, in fact, be employed as an indicator of the evolutionary stages of the hydrothermal cycle. At the same time, the predominance of Fe oxi-hydroxides at the Active TAG mound likely suggests an increase in the supply of this material to the modern sediments. An analogous stage occurred about 7 ka BP. Figure 9 demonstrates that the period of time corresponding to the reactivation of the spring was predated by a drastic increase in the outflow of hydrothermal Fe [29].

If the reasoning presented above is correct, then the evolution of the hydrothermal–sedimentary material within a single hydrothermal cycle 3 to 6 ka long can be imagined as follows. The attenuation of volcanic activity is associated with faulting and fracturing in the oceanic crust, which facilitates the development of a hydrothermal convection system and its rapid evolution. For example, the 1993–1996 research at the Lucky Strike and Menez Gwen fields (37°17′N and 37°50′N at MAR, respectively) [52, 53] have demonstrated that changes affected not only the temperature of the solutions but also their gas composition (first of all, H_2S) and the concentrations of chemical elements over a time span as brief as a few years. Analogous data on the F spring at the very young crust at the East Pacific Rise (EPR) at 9°16.8′N also display remarkable evolutionary changes in the composition of the fluid between 1991 and 1994 [54]. The reasons for these fluctuations remain obscure and can be related to the evolution of the circulation system, which is controlled by the evo-

lution of the magmatic and tectonic processes. The discharge zone of hydrothermal solutions (hydrothermal field) was then controlled by the structural pattern of tectonic fractures and faults, and single hydrothermal edifices started to grow on the seafloor surface. In the process of their growth and the sealing of minor fluid conduits with hydrothermal material, the discharge zone narrowed, which led to the development of a significant central spring. Its activity gradually also decreased with time and eventually ceased. The periodical reactivation of some edifices could be related to their destruction under the effect of the increasing pressure of hydrothermal solutions. An analogy is the closing of a faucet: the hydrodynamic wave occurs then in resonance and thus manyfold increases the hydrodynamic shock. The destruction mechanism of vertical edifices was described in much detail in the literature based on extensive factual material on ore clastic rocks, which are widespread at modern hydrothermal fields. The cessation of hydrothermal activity may also be affected by the resumption of local volcanic activity. Liquid basic lavas obviously could seal and block fractures and cracks that had served as conduits for hydrothermal solutions. The hydrothermal system passes to the state of an interlude before the next hydrothermal cycle.

The periodical recurrence of these cycles results in the extension and deepening of the fracturing zone in the basement under the effect of tectonic and hydrodynamic processes and in the gradual extension of the hydrothermal orebody itself both on the seafloor surface and down the underlying subore rocks. The focusing of solution discharge and the development of a single significant conduit leads, in turn, to the development of the subsurface circulation of solutions (effect of an aspirator) in the zone of brecciated and shattered subore rocks. Thus, the zone where the fluid mixed with seawater also deepened, and the mineral-forming process proceeds more smoothly, in contrast to this process at young vents, whose basement is still not extensively shattered. Indirect evidence in support of this idea is the low pyrrhotite contents in the smokes of the Active TAG mound, which possesses a well-developed system of roots. A condition necessary for pyrrhotite precipitation from a solution is known to be the reaction rate: the higher this rate, the higher the probability of pyrrhotite crystallization. Pyrrhotite usually precipitates in the zone of the maximum oversaturation of the solution at contact between the hot fluid and seawater.

The attenuation of hydrothermal activity at the TAG field within a single hydrothermal cycle, a phenomenon inferred from several lines of indirect evidence [29], should have inevitably bring about exogenic processes, so that the process itself should have gradually become supergene. The example of modern submarine edifices and ancient sulfide orebodies also demonstrates that the resumption of hydrothermal activity develops toward a decrease in the degree of oxidation of the ores composing the edifice, and the cessation (supergene phase) leads, conversely, to an increase in this degree. For example, corresponding to the degree of oxidation, Fe-bearing minerals can be arranged in the following succession: $Fe^{2+}S$ (trolilite)—$Fe^{2+}_{(1-x)}S$ (pyrrhotite)—$Fe^{2+}S_2$ (pyrite, marcasite)—$Fe^{2+}Fe^{3+}_2O_4$ (magnetite)—$Fe^{3+}O(OH)$ (goethite)—$Fe^{3+}_2O_3$ (hematite). Young springs are characterized by reducing conditions and a pyrite–pyrrhotite composition of the smokes of their smoker. As the activity of the spring gradually attenuates, the mineral composition of the edifice and, correspondingly, of the hydrothermal–sedimentary material carried by the spring to the surface, should systematically change to pyrite–oxi-hydroxide, thus reflecting of the involvement of exogenic processes. An important role is played there by the shattering of the subore rocks (basement of the edifice) and the extension of the mixing zone of the solutions with seawater (see above). Sulfide particles carried by a spring usually precipitate within a few dozen (rarely, a few hundred) meters from it, whereas Fe oxi-hydroxides can migrate (because of their smaller grain sizes) for much greater distances with water masses and accumulate outside the hydrothermal edifices, forming both proximal and distal metalliferous sediments.

Thus, there can be several reasons for high contents of oxidized Fe species in the sedimentary material of the TAG edifice. First, the accumulation of ore material is associated with the development of sulfide roots (stockwork sulfide ores) in the basement of the edifice. As was mentioned above, the mature TAG edifice has roots extending for at least 125 m down the basaltic basement. Thus, the precipitation of ore material from the solutions starts long before these solutions reach the vent. Consequently, the smokes of the smoker contain only the remaining ore minerals, which are depleted in S (Fe > S). The latter was partly spent on sulfide minerals according to reactions like (1), (3), and (4). Second, it should be taken into account that the evolution of a recycling hydrothermal system is accompanied by the evolutionary transformations in the composition of the solutions feeding this body, because various chemical elements are variably scavenged from the rocks of the crystalline basement. The relation Fe $\ll$ S in a young spring should eventually give way to Fe > S in a mature one [1]. Third, previously deposited elements can be remobilized from the orebody by the ascending solution flow, as was documented, for example, for Fe and Zn, according to reactions (6) and (7).

Comparative analysis of the chemical composition of the hydrothermal–sedimentary material, hydrothermal solutions, and tholeiitic basalts. It is known that a result of interactions between seawater and basalts is the leaching of 8–16% of the mass of these rocks. The removal of Si accounts for approximately half of the loss, Ca accounts for one-fifth of it, and the removal of all other elements corresponds to

10% for each of them [55]. Currently available extensive material on the chemistry of hydrothermal solutions reveals their characteristic similarities throughout the whole oceanic rift system. This, in turn, led to the classing of all known hydrothermal ore occurrences with a single metallogenetic province of the Earth and, consequently, to consider all of these processes on a global scale. Their principal differences from ambient seawater are ubiquitously low pH values (2–6, 3.3–3.8 on average), reducing conditions, absence of Mg, SO_4^{2-}, dissolved O_2 and U, and high concentrations of metals and H_2S (Table 3). However, in spite of these similarities, the composition of the hydrothermal solutions of the springs considered here show certain differences, which are also reflected in the composition of their hydrothermal–sedimentary material.

The Cu/Fe ratio in both the solution and the sedimentary material at the TAG field is higher than at Broken Spur (Table 6), which can account for the mobility of Cu relative to Fe during their leaching from volcanic rocks. The ratios in the solution and sedimentary material are very close and testify to the high efficiency of Cu precipitation near the spring. The Zn/Fe ratio in solution near the spring at the Broken Spur field is higher than at TAG. However, the trap material of the TAG field has a higher Zn/Fe ratio, which testifies to its active precipitation from the solution in the form of sphalerite. The Zn/Fe ratio of the solution and sedimentary material at the Broken Spur spring field is higher than at TAG spring, a fact confirming the more active removal of Zn relative to Cu at the younger field. The Zn/Cu and Zn/Fe ratios are the highest in the solution of the spring at 21°N at EPR. The higher Ca concentrations in the hydrothermal solutions relative to Fe predetermine high Ca/Fe ratios. The contrastingly low ratios in the sedimentary material testify to weak Ca involvement in the mineral-forming processes (low efficiency of precipitation). No more than a few percent of the total Ca concentration is spent on the crystallization of anhydrite (near the vent), and even less Ca is incorporated into hydrothermal aragonite (in the ascending parts of the plume). The bulk of Ca is supplied to bottom oceanic waters in the form of solutions. The same pertains to Si. However, the higher mobility of Ca caused a higher Ca/Fe ratio in the sedimentary material of the young spring than in the mature one, and the Si/Fe ratio is, conversely, higher at TAG than at the Broken Spur, perhaps because of the higher resistance of aluminosilicates to leaching. The Al/Fe ratio in solutions is higher than in the sedimentary material, which suggests weak Al participation in the mineral-forming processes. Because of the high Al stability in the rocks, the Al/Fe ratios at both fields are virtually identical.

The chemical composition of the trap material also shows high contents of ore metals, which predetermines their high enrichment coefficients (EC) relative to the composition of tholeiitic basalts from which these elements are leached: Cu, Zn (thousands), Fe, Co (hundreds), As (thousands), and Sb, Ba, and P (hundreds) (Table 7). In spite of the aforementioned similarities, the fields show some differences. For example, the higher Cu, As, Co, Sb, Ba, P, and Si contents in the trap material from the TAG field predetermine the higher enrichment coefficients of these elements (Fig. 10).

Table 7. Enrichment coefficients (relative to tholeiitic basalts as the parental rock) of chemical elements in trap material collected beneath the smoke of black smokers at the Broken Spur (BS) and TAG fields. The coefficients were calculated by the formula EC = (Element/Al) in trap/(Element/Al) in basalt

Chemical element	Enrichment coefficient (EC)	
	BS	TAG
Se	480000	99299
Cu	6520	8644
Zn	4785	4919
As	2170	6677
Co	460	820
Fe	298	361
Sb	213	404
Ba	190	449
P	126	217
Ca	41	9.9
Si	1.4	7.4

Note: Concentrations of chemical elements in tholeiitic basalts are compiled from [28].

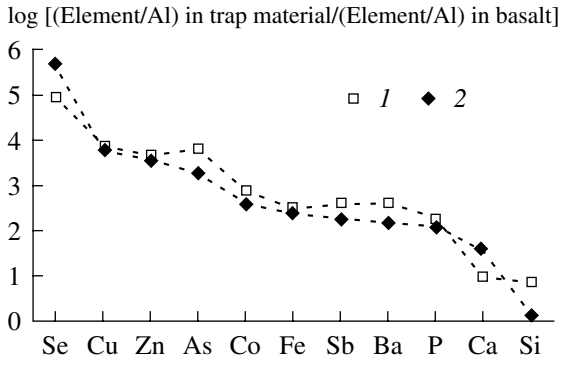

Fig. 10. Element diagram for trap material from the TAG and Broken Spur hydrothermal fields (element concentrations are normalized to their contents in average oceanic tholeiitic basalt). (*1*) TAG and (*2*) Broken Spur.

This is caused, first of all, by the significant supply of these elements with primary metalliferous solutions at the TAG field (Table 3). The highest differences between EC in the trap material from the springs are typical of Se (by a factor of 4.8), As (by a factor of 3), Ca (4.1), and Si (5.2). The EC of Se and Ca are higher at the Broken Spur field, and those of As and Si are higher at TAG. This suggests that the composition of the hydrothermal–sedimentary material is closely related to the composition of hydrothermal solutions.

CONCLUSIONS

1. The origin of hydrothermal–sedimentary material is a complicated multistage process, which is closely related to the formation of colloid solutions, the coagulation of their dispersed phase, and sorption–adsorption processes. Detailed data obtained on the mineral assemblages and textures of this material indicate that the material started to form inside the orebody or below it, in the subore rocks, but not only in the discharge zone of fluid from the vent of the spring, as was thought previously.

2. It is important to stress that the composition of the hydrothermal–sedimentary material (its granulometry, mineralogy, and chemistry) is closely related to certain evolutionary stages of the mineral-forming process and reflects the composition of the primary metalliferous solutions and the influence of hydrothermal and supergene processes. This composition can be used as an indicator when the evolutionary history of hydrothermal activity is studied.

3. The assessment of the fluxes of hydrothermal–sedimentary material with the use of sediment traps near springs allowed us to reveal the inner structure of the flow and determine its contribution to the ore-forming processes.

ACKNOWLEDGMENTS

The author thanks E.S. Chernyaev, the pilot of the Mir submersible for help in obtaining the factual material, and V.N. Apollonov (Institute of the Geology of Ore Deposits, Petrography, Mineralogy, and Geochemistry, Russian Academy of Sciences) for help with the processing of this material. This study was supported by the Joint Russian–American Program "Basic Research and Higher Education" (BRHE); the Macarthur, Carnegie, and CRDF foundations; and the Federal Agency for Education of the Russian Federation.

REFERENCES

1. D. V. Grichuk, E. E. Abramova, and A. V. Tutubalin, "A Thermodynamic Model of a Submarine Massive Sulfide Formation in a Convecting Hydrothermal System," Geol. Rudn. Mestorozhd. **40** (1), 3–19 (1998) [Geol. Ore Dep. **40**, 1–15 (1998)].
2. A. P. Lisitsyn, "Hydrothermal Systems of the World Ocean: Input of Endogenous Material," in *Hydrothermal Systems and Sedimentary Formations of the Atlantic Mid-Ocean Ridges* (Nauka, Moscow, 1993), pp. 147–245 [in Russian].
3. M. B. Borodaevskaya, D. I. Gorzhevskii, A. I. Krivtsov, et al., *Sulfide Deposits around the World* (Nedra, Moscow, 1979) [in Russian].
4. R. A. Feely, M. Lewison, G. J. Massoth, et al., "Composition and Dissolution of Black Smoker Particulate from Active Vents on the Juan de Fuca Ridge," J. Geophys. Res. **90** (B11), 11347–11363 (1987).
5. R. A. Feely, G. J. Massoth, J. H. Trefry, et al., "Composition and Sedimentation of Hydrothermal Plume Particles from North Cleft Segment, Juan de Fuca Ridge," J. Geophys. Res. **99** (B3), 4985–5006 (1994).
6. J. Dymond and S. Roth, "Plume Dispersed Hydrothermal Particles: A Time-Series Record of Settling Flux from the Endevor Ridge Using Moored Sensors," Geochim. Cosmochim. Acta **52**, 2525–2536 (1988).
7. M. J. Mottl and T. E. McConachy, "Chemical Processes in Buoyant Hydrothermal Plumes on the East Pacific Rise Near 21°N," Geochim. Cosmochim. Acta **54**, 1911–1927 (1990).
8. A. Khripounoff and P. Alberic, "Settling of Particles in a Hydrothermal Vent Field (East Pacific Rise 13°N) Measured with Sediment Traps," Deep.-Sea Res. **38** (6), 729–744 (1991).
9. "BRAVEX-94 Scientific Team, BRAVEX-94: a Joint British–Russian Expedition to the Broken Spur and TAG Hydrothermal Vent Sites on the Mid-Atlantic Ridge," BRIDGE Newsletter, No. 7, 6–9 (1994).
10. V. N. Lukashin, V. Yu. Rusakov, A. P. Lisitzin, et al., "Study of Particle Fluxes in the Broken Spur Hydrothermal Vent Field (29°N, Mid-Atlantic Ridge)," Explor. Mining Geol. **8** (3) (1999).
11. V. N. Lukashin, V. Yu. Rusakov, A. P. Lisitsyn, et al., "Particle Fluxes, Mineralogy, and Chemistry of Sedimentary Material in the Broken Spur Hydrothermal Field, Mid-Atlantic Ridge, 29°N," Geokhimiya, No. 4, 370–382 (2000) [Geochem. Int. **38**, 331–342 (2000)].
12. G. A. Cherkashev, Extended Abstract of Doctoral Dissertation in Geology and Mineralogy (St. Petersburg, 2004).
13. R. W. Nesbitt and B. J. Murton, "Chimney Growth Rate and Metal Deposition at the Broken Spur Vent Field, 29°N, MAR: A Correction and Further Speculation," BRIDGE Newsletter, No. 9, 38–41 (1995).
14. Yu. A. Bogdanov, N. S. Bortnikov, and A. P. Lisitsyn, "The Origin of the Hydrothermal Sulfide Ores in the Axial Parts of the Mid-Atlantic Ridge," Geol. Rudn. Mestorozhd. **39**, 409–429 (1997) [Geol. Ore Dep. **39**, 351–370 (1997)].
15. S. E. Humphris, P. M. Herzing, D. J. Miller, et al., "The Internal Structure of An Active Sea-Floor Massive Sulphide Deposit," Nature **377**, 713–716 (1995).
16. C. Laloeu, G. Thompson, M. Arnold, et al., "Geochronology of TAG and Snake Pit Hydrothermal Fields, Mid-Atlantic Ridge: Witness to a Long and Complex Hydrothermal History," Earth Planet. Sci. Lett. **97**, 113–128 (1990).

17. C. Laloeu, J. L. Reyss, E. Brichet, et al., "New Age Data for Mid-Atlantic Ridge Hydrothermal Site: TAG and Snake Pit Chronology Revisited," J. Geophys. Res. **98**, 9705–9713 (1993).
18. C. Laloeu, J. L. Reyss, E. Brichet, et al., "Hydrothermal Activity on 10-Years Scale at a Slow-Spreading Ridge, TAG Hydrothermal Field, Mid-Atlantic Ridge 26°N" J. Geophys. Res. **100** (B9), 17855–17862 (1995).
19. V. Yu. Rusakov, V. N. Lukashin, and A. A. Burovkin, "A Sediment Trap for Short-Term Studies of Vertical Particle Fluxes in the Ocean," Okeanologiya **36**, 798–800 (1996) [Oceanology **36**, 754–756 (1996)].
20. B. J. Murton and C. Van Dover, ""Alvin" Dives on the Broken Spur Hydrothermal Vent Field at 29°10'N on the Mid-Atlantic Ridge," BRIDGE Newsletter **5**, 11–14 (1993).
21. G. Fischer and G. Wefer, "Sampling, Preparation and Analysis of Marine Particulate Matter," in *Marine Particles: Analysis and Characterization*, Geophys. Monograph. **63**, 391–397 (1991).
22. M. J. Murton, C. Van Dover, and E. Southward, "Geological Setting and Ecology of the Broken Spur Hydrothermal Vent Field: 29°10′N on the Mid-Atlantic Ridge," in *Hydrothermal Vents and Processes*, Spec. Publ. Geol. Soc. London **87**, 33–41 (1995).
23. J. M. Edmond, A. C. Campbell, M. P. Palmer, and C. German, "Geochemistry of Hydrothermal Fluids from the Mid-Atlantic Ridge: TAG and MARK," EOS (AGU) **71**, 1650–1651 (1990).
24. A. C. Campbell, M. R. Palmer, G. P. Klinkhammer, et al., "Chemistry of Hot Springs on the Mid-Atlantic Ridge," Nature **335** (6190), 514–519 (1988).
25. K. L. von Damm, J. M. Edmond, B. Grant, et al., "Chemistry of Submarine Hydrothermal Solutions at 21°N, East Pacific Rise," Geochim. Cosmochim. Acta **49** (11), 2197–2220 (1985).
26. R. Haymon and M. Kastner, "Hot Spring Deposits on the East Pacific Rise at 21°N: Preliminary Description of Mineralogy and Genesis," Earth Planet. Sci. Lett. **53**, 363–381 (1981).
27. E. A. Romankevich, *Geochemistry of Organic Matter in the Ocean* (Springer–Verlag, Berlin–New York, 1984.
28. G. V. Voitkevich, A. V. Kokin, A. E. Miroshnikov, and V. G. Prokhorov, *Reference Book on Geochemistry* (Nedra, Moscow, 1990) [in Russian].
29. Yu. A. Bogdanov, *Hydrothermal Occurrences of Mid-Atlantic Ridge Rifts* (Nauchnyi Mir, Moscow, 1997) [in Russian].
30. J. B. Butler and R. W. Nesbitt, "Hydrothermal Sulfides from the Broken Spur Vent Field, 29°10′ N Mid-Atlantic Ridge: Preliminary Observations," BRIDGE Newsletter, No. 9, 24–28 (1995).
31. R. C. Duckworth, R. Knott, A. E. Fallick, et al., "Mineralogy and Sulfur Isotope Geochemistry of the Broken Spur Sulfides, 29°N Mid-Atlantic Ridge," in *Hydrothermal Vents and Processes*, Ed. by L. M. Parson, C. L. Walker, and R. D. Dixon, Spec. Publ. Geol. Soc. London. **87**, 175–189 (1995).
32. E. G. Gurvich, *Metalliferous Sediments of the World's Ocean* (Nauchnyi Mir, Moscow, 1998) [in Russian].
33. A. L. Vereshchaka and V. E. Vinogradov, "Three-Dimensional View of the Atlantic Abyssal Benthopelagic Vent Community," Cah. Biol. Mar. **43**, 303–305 (2002).
34. D. V. Grichuk, *Thermodynamic Models of Submarine Hydrothermal Systems* (Nauchnyi Mir, Moscow, 2000) [in Russian].
35. S. G. Krasnov, G. A. Cherkashev, T. V. Stepanova, et al., "Detailed Geological Studies of Hydrothermal Fields in the North Atlantic," in *Hydrothermal Vents and Processes*, Ed. by L. M. Parson, C. L. Walker, and R. D. Dixon, Spec. Publ. Geol. Soc. London. **87**, 175–189 (1995).
36. M. K. Tivey, S. E. Humphris, G. Thompson, et al., "Deducing Patterns of Fluid Flow and Mixing within the Active TAG Hydrothermal Mound Using Mineralogical and Geochemical Data," J. Geophys. Res. **100**, 12527–12555 (1995).
37. M. D. Hannington, P. M. Herzig, S. D. Scott, et al., "Comparative Mineralogy and Geochemistry of Gold-Bearing Sulfide Deposits on the Mid-Ocean Ridge," Mar. Geol. **101**, 217–248 (1991).
38. A. I. Krivtsov, O. V. Minina, A. G. Volochkov, et al., *Sulfide Deposits. Series: Models of the Noble and Base Metal Deposits* (TsNIGRI, Moscow, 2002) [in Russian].
39. V. Yu. Rusakov, Extended Abstract of Candidate's Dissertation in Geology and Mineralogy (Moscow, 2002).
40. M. D. Rudnicki, *Hydrothermal Plumes at the Mid-Atlantic Ridge*. PhD Thesis. (Cambridge Univ., Cambridge, 1990).
41. V. Yu. Rusakov, "Flux and Precipitation of Hydrothermal Iron in Rift Valley at 26° and 29°N Mid-Atlantic Ridge," Okeanologiya, 2007 (in press).
42. D. R. Janecky and I. Shanks II, "Computational Modeling of Chemical and Sulfur Isotopic Reaction Processes in Seafloor Hydrothermal Systems: Chimneys, Massive Sulfides, and Subjacent Alteration Zones," Can. Mineral. **26**, 805–825 (1988).
43. M. D. Rudnicki and H. Elderfield, "A Chemical Model of the Buoyant and Neutrally Buoyant Plume Above the TAG Vent Field, 26 Degree N, Mid-Atlantic Ridge," Geochim. Cosmochim. Acta **57**, 2939–2957 (1993).
44. V. V. Kuznetsov, *Physical and Colloidal Chemistry* (Vysshaya Shkola, Moscow, 1968) [in Russian].
45. A. G. Betekhtin, F. I. Vol'fson, A. N. Zavaritskii, et al., *Principal Problems in the Theory of Magmatic Ore Deposits* (AN SSSR, Moscow, 1953) [in Russian].
46. N. N. Mozgova, Yu. S. Borodaev, I. F. Gablina, et al., "Mineral Assemblages as Indicators of the Maturity of Oceanic Hydrothermal Sulfide Mounds," Litol. Polezn. Iskop., No. 4, 339–367 (2005) [Lithol. Miner. Resour. **40**, 293–319 (2005)].
47. J. B. Murowchick and H. L. Barnes, "Marcasite Precipitation from Hydrothermal Solution," Geochim. Cosmochim. Acta **50** (12), 2615–2629 (1986).
48. Yu. A. Bogdanov, N. S. Bortnikov, I. V. Vikent'ev, et al., "A New Type of Modern Mineral-Forming Systems: Black Smokers of the Hydrothermal Field at 14°45′N Latitude, Mid-Atlantic Ridge," Geol. Rudn. Mestorozhd. **39**, 68–90 (1997) [Geol. Ore Dep. **39**, 58–78 (1997)].
49. C. R. German and R. S. J. Sparks, "Particle Recycling in the TAG Hydrothermal Plume," Earth Planet. Sci. Lett **116**, 129–134 (1993).

50. M. D. Hannington and I. R. Jonasson, "Physical and Chemical Processes of Mid-Ocean Ridges," in *Seafloor Hydrothermal Systems: Physical, Chemical, Biological, and Geological Interactions*, Geophys. Monograph. **91**, 115–156 (1995).

51. A. P. Lisitsyn, Yu. A. Bogdanov, L. P. Zonenshain, et al., "Hydrothermal Occurrences of Mid-Atlantic Ridge at 26°N (TAG Hydrothermal Field)," Izv. Akad. Nauk SSSR, Ser. Geol., No. 12, 3–20 (1989).

52. K. L. von Damm, A. M. Bray, L. G. Buttermore, and S. E. Oosting, "The Geochemical Controls on Vent Fluids from the Lucky Strike Vent Field, Mid-Atlantic Ridge," Earth Planet. Sci. Lett. **160**, 521–536 (1998).

53. J. L. Charlou, J. P. Donval, E. Douville, et al., "Compared Geochemical Signatures and the Evolution of Menez Gwen (37°50′N) and Lucky Strike (37°17′N) Hydrothermal Fluids, South of the Azores Triple Junction on the Mid-Atlantic Ridge," Chem. Geol., No. 171, 49–75 (2000).

54. K. L. von Damm, L. G. Buttermore, S. E. Oosting, et al., "Direct Observation of the Evolution of a Seafloor 'Black Smoker' from Vapor to Brine," Earth Planet. Sci. Lett. **149**, 101–111 (1997).

55. A. P. Lisitsyn, Yu. A. Bogdanov, and E. G. Gurvich, *Hydrothermal Rocks of the Oceanic Rift Zones* (Nauka, Moscow, 1990) [in Russian].